REPORT DOCUMENTATION PAGE

Form Approved OMB NO. 0704-0188

1. REPORT DATE (DD-MM-YYYY)	2. REPORT TYPE	3. DATES COVERED (From - To)
04-07-2008	Final Report	19-Apr-2004 - 18-Apr-2008

4. TITLE AND SUBTITLE
Destruction Chemistry of Mustard Simulants

5a. CONTRACT NUMBER
W911NF-04-1-0120

5b. GRANT NUMBER

5c. PROGRAM ELEMENT NUMBER
611102

6. AUTHORS
J.W. Bozzelli, E. M. Fisher, F.C. Gouldin

5d. PROJECT NUMBER

5e. TASK NUMBER

5f. WORK UNIT NUMBER

7. PERFORMING ORGANIZATION NAMES AND ADDRESSES
Cornell University
Office of Sponsored Programs
Cornell University
Ithaca, NY 14853 -2801

8. PERFORMING ORGANIZATION REPORT NUMBER

9. SPONSORING/MONITORING AGENCY NAME(S) AND ADDRESS(ES)
U.S. Army Research Office
P.O. Box 12211
Research Triangle Park, NC 27709-2211

10. SPONSOR/MONITOR'S ACRONYM(S)
ARO

11. SPONSOR/MONITOR'S REPORT NUMBER(S)
45844-CH.2

12. DISTRIBUTION AVAILIBILITY STATEMENT
Approved for Public Release; Distribution Unlimited

13. SUPPLEMENTARY NOTES
The views, opinions and/or findings contained in this report are those of the author(s) and should not contrued as an official Department of the Army position, policy or decision, unless so designated by other documentation.

14. ABSTRACT

This study investigates the destruction chemistry of organosulfur compounds under both pyrolytic and oxidative conditions. We focus on the destruction of alkyl sulfides that are surrogates for chemical warfare agents H, HD, and HT. We report our work on developing thermochemistry, reaction pathways and kinetic parameters for multiple chemical subsystems, using computational chemistry methods. We also report our experimental results from flow reactor experiments for pyrolysis and oxidation of two alkyl sulfides: diethyl sulfide and ethyl methyl sulfide. A detailed, elementary reaction, mechanism has been

15. SUBJECT TERMS
organosulfur, oxidation, pyrolysis, chemical kinetic mechanism, thermochemistry, reaction, kinetics, flow reactor, GC/MS, FTIR, mustard agent simulant, CWA simulant

16. SECURITY CLASSIFICATION OF:			17. LIMITATION OF ABSTRACT	15. NUMBER OF PAGES	19a. NAME OF RESPONSIBLE PERSON
a. REPORT	b. ABSTRACT	c. THIS PAGE			Elizabeth Fisher
U	U	U	SAR		19b. TELEPHONE NUMBER 607-255-8309

Report Title

Destruction Chemistry of Mustard Simulants

ABSTRACT

This study investigates the destruction chemistry of organosulfur compounds under both pyrolytic and oxidative conditions. We focus on the destruction of alkyl sulfides that are surrogates for chemical warfare agents H, HD, and HT. We report our work on developing thermochemistry, reaction pathways and kinetic parameters for multiple chemical subsystems, using computational chemistry methods. We also report our experimental results from flow reactor experiments for pyrolysis and oxidation of two alkyl sulfides: diethyl sulfide and ethyl methyl sulfide. A detailed, elementary reaction, mechanism has been developed to describe the pyrolysis and oxidation chemistry relevant to these compounds.

List of papers submitted or published that acknowledge ARO support during this reporting period. List the papers, including journal references, in the following categories:

(a) Papers published in peer-reviewed journals (N/A for none)

X. Zheng, E.M. Fisher, F.C. Gouldin, L. Zhu, and J.W. Bozzelli, 2008, "Experimental and Computational Study of Diethyl Sulfide Pyrolysis and Mechanism," accepted for publication, Proceedings of the Combustion Institute, v. 32, 2008.

"Quantum chemical study of the structure and thermochemistry of the five-membered nitrogen-containing heterocycles and their anions and radicals,"
Da Silva, Gabriel; Moore, Eric E.; Bozzelli, Joseph W., Journal of Physical Chemistry A, v 110, n 51, Dec 28, 2006, p 13979-13988

"Formation of a Criegee intermediate in the low-temperature oxidation of dimethyl sulfoxide,"
Asatryan R, Bozzelli JW., PHYSICAL CHEMISTRY CHEMICAL PHYSICS Volume: 10, Issue: 13, Pages: 1769-1780, 2008.

"Thermochemistry of oxabicycloheptenes: Enthalpy of formation, entropy and heat capacity,"
Bozzelli, Joseph W.; Rajasekaran, Indumathi; Hur, Jin, Journal of Physical Organic Chemistry, v 19, n 2, February, 2006, p 93-103

"Thermochemistry of oxabicyclo-heptanes, oxabicyclo-heptene: Enthalpy of formation, entropy, heat capacity, and group additivity,"
Bozzelli JW, Rajasekaran I, JOURNAL OF PHYSICAL AND CHEMICAL REFERENCE DATA Volume: 36 Issue: 2 Pages: 663-681 JUN 2007.

"Thermochemistry for enthalpies and reaction paths of nitrous acid isomers,"
Asatryan, Rubik; Bozzelli, Joseph W.; Simmie, John M., International Journal of Chemical Kinetics, v 39, n 7, July, 2007, p 378-398

"The multi-channel reaction of CH3S+O-3(2): Thermochemistry and kinetic barriers,"
Zhu L, Bozzelli JW, JOURNAL OF MOLECULAR STRUCTURE-THEOCHEM Volume: 728 Issue: 1-3 Pages: 147-157 SEP 2 2005.

"Kinetics of the multichannel reaction of methanethiyl radical (CH3S center dot) with O-3(2)"
Author(s): Zhu L, Bozzelli JW
Source: JOURNAL OF PHYSICAL CHEMISTRY A Volume: 110 Issue: 21 Pages: 6923-6937 Published: JUN 1 2006

Number of Papers published in peer-reviewed journals: 8.00

(b) Papers published in non-peer-reviewed journals or in conference proceedings (N/A for none)

Number of Papers published in non peer-reviewed journals: 0.00

(c) Presentations

Xin Zheng, E. M. Fisher, F. C. Gouldin, Li Zhu, and J.W. Bozzelli, “Flow Reactor Pyrolysis of Diethyl Sulfide,” presented at the 2007 Fall Meeting of the Eastern States Section of the Combustion Institute, October 2007, Charlottesville, VA.

R. Asatryan and J.W. Bozzelli, "Theoretical Study on Thiyl Reactions with Carbon Monoxide: RS.+CO," Poster at Northeast Regional ACS Meeting, Binghamton, NY, Fall 2006.

Xin Zheng, E. M. Fisher, F. C. Gouldin, Li Zhu, J.W. Bozzelli, “Flow Reactor Pyrolysis of Diethyl Sulfide,” presented at the 2005 Fall Meeting of the Western States Section of the Combustion Institute, October 2005, Stanford, CA.

"Thermochemical and kinetic analysis on decomposition and oxidation of sulfur hydrocarbons."
Jin F, Bozzelli JW, Zhu L, et al., ABSTRACTS OF PAPERS OF THE AMERICAN CHEMICAL SOCIETY Volume: 228 Page U257 Part 2 Meeting Abstract: 379-PHYS, AUG 22 2004.

"Reaction paths, kinetics and thermochemical properties on reaction of methylthiol (CH3SH) and dimethylsulfide (CH3SCH3) radicals with O2."
Jin F, Zhu L, Bozzelli JW, ABSTRACTS OF PAPERS OF THE AMERICAN CHEMICAL SOCIETY Volume: 228 Page U259 Part 2 Meeting Abstract: 391-PHYS, AUG 22 2004

"Reaction paths, kinetics and thermochemical properties in the dimethylsulfide radical reaction with O2: CH3SC center dot H2+O2."
Bozzelli JW, Jin F, ABSTRACTS OF PAPERS OF THE AMERICAN CHEMICAL SOCIETY Volume: 227 Pages U1099 Part 1 Meeting Abstract: 192-FUEL MAR 28 2004

"Thermochemical Properties (Enthalpy, Entropy and Heat Capacity), Rotation Barriers, Bond Energies of CH3SCH2CH=O, CH3SC(CH3)=O, CH3SCH=O, HSC(CH3)=O, HSCH2C(CH3)=O, HSCH=O, HSCH2CH=O and CH3SCH2C(CH3)=O" David N. Nare, Shyam G. Patel and Joseph W. Bozzelli, AIChE International Meeting, Undergraduate Research, Indianapolis, Indiana, November 2004, also Honor Students Undergraduate Research Conference – Toronto, Canada, Nov 18, 2004

Number of Presentations: 7.00

Non Peer-Reviewed Conference Proceeding publications (other than abstracts):

"Reaction paths, kinetics, and thermochemical properties on the thioformyl radical (S=C.H) with O2 reaction," Li Zhu and J. W. Bozzelli, 5th US Combustion Meeting, The Combustion Institute, UCSD, March 25-28, 2007.

"Reaction paths, kinetics, and thermochemical properties on reaction of methylthiyl (CH3S) and methylthiomethyl (CH3SCH2) radicals with O2," Li Zhu, Fei Jin, and J.W. Bozzelli, Extended Abstracts International Gas Kinetics Conference, Orleans, France July 22-28, 2006 (Oral presentation).

"Thermochemical properties, reaction paths, and kinetics of secondary vinylic radicals in C4 to C7 1,3-diene systems and their reactions with O2," Leonhard Rutzl, Gabriel da Silva, Joseph Bozzelli, and Henning Bockhorn, Extended Abstracts International Gas Kinetics Conference, Orleans, France July 22-28, 2006 (Poster).

"Toluene combustion: reaction paths thermochemical properties, and kinetic analysis on teh methylphenyl. 1 radical + O2 reaction pathways," Gabriel da Silva, Chiung-Chu Chen, Joseph Bozzelli, Tim Barckholtz, and John T. Farrell, Extended Abstracts International Gas Kinetics Conference, Orleans, France July 22-28, 2006 (Poster).

"A computational study on kinetics and thermochemistry of acetone and acetone radical oxidation," Ahmed M. El-Nahas, Joseph Bozzelli, Henry Curran, John Simmie, Guillaume Vanhove, and Grainne Black, Extended Abstracts International Gas Kinetics Conference, Orleans, France July 22-28, 2006 (Oral Presentation).

"Thermochemistry, kinetics and kinetic modeling on atmospheric reactions of the benzene-OH adduct with O2," Chiung-Chu Chen and Joseph Bozzelli, Extended Abstracts International Gas Kinetics Conference, Orleans, France July 22-28, 2006 (Poster).

"Oxidation path of dimethyl sulfoxide results in direct exothermic formation of Criegee Intermediate," Rubik Asatryan and Joseph Bozzelli, Extended Abstracts International Gas Kinetics Conference, Orleans, France July 22-28, 2006 (Poster).

"Reaction paths, kinetics and thermochemical properties on reaction of methylthiyl (CH3S) and methylthiomethyl (CH3SCH2) radicals with O2
Li Zhu, Fei Jin and Joseph W. Bozzelli" Extended Abstracts Nist International Kinetics conference, Gaithersburg, Md July 25 – 29 2005

"Reaction paths, kinetics and thermochemical properties on reaction of methylthiyl (CH3S) and methylthiomethyl (CH3SCH2) radicals with O2," Li Zhu, Fei Jin and Joseph W. Bozzelli* 4th US meeting of the Combustion Institute, Drexel Univeristy, Phila Penna, 2005

Number of Non Peer-Reviewed Conference Proceeding publications (other than abstracts): 9

Peer-Reviewed Conference Proceeding publications (other than abstracts):

Number of Peer-Reviewed Conference Proceeding publications (other than abstracts): 0

(d) Manuscripts

Number of Manuscripts: 0.00

Number of Inventions:

Graduate Students

NAME	PERCENT_SUPPORTED
Xin Zheng	0.75
John Cole	0.04
FTE Equivalent:	**0.79**
Total Number:	**2**

Names of Post Doctorates

NAME	PERCENT_SUPPORTED
Ponmile Oloyede	0.03
Li Zhu	0.65
Rubik Asatryan	0.38
FTE Equivalent:	**1.06**
Total Number:	**3**

Names of Faculty Supported

NAME	PERCENT_SUPPORTED	National Academy Member
Joseph Bozzelli	0.01	No
Frederick Gouldin	0.01	No
Elizabeth Fisher	0.01	No
FTE Equivalent:	**0.03**	
Total Number:	**3**	

Names of Under Graduate students supported

NAME	PERCENT_SUPPORTED
Adam Gross	0.00
David Nare	0.01
Ariel Ravel	0.00
Stephen Istivan	0.00
Kathy Alberco	0.00
Shyam Patel	0.01
FTE Equivalent:	**0.02**
Total Number:	**6**

Student Metrics

This section only applies to graduating undergraduates supported by this agreement in this reporting period

The number of undergraduates funded by this agreement who graduated during this period:	6.00
The number of undergraduates funded by this agreement who graduated during this period with a degree in science, mathematics, engineering, or technology fields:.....	6.00
The number of undergraduates funded by your agreement who graduated during this period and will continue to pursue a graduate or Ph.D. degree in science, mathematics, engineering, or technology fields:.....	2.00
Number of graduating undergraduates who achieved a 3.5 GPA to 4.0 (4.0 max scale):	4.00
Number of graduating undergraduates funded by a DoD funded Center of Excellence grant for Education, Research and Engineering:	0.00
The number of undergraduates funded by your agreement who graduated during this period and intend to work for the Department of Defense	0.00
The number of undergraduates funded by your agreement who graduated during this period and will receive scholarships or fellowships for further studies in science, mathematics, engineering or technology fields:	1.00

Names of Personnel receiving masters degrees

NAME
Total Number:

Names of personnel receiving PHDs

NAME
Total Number:

Names of other research staff

NAME	PERCENT_SUPPORTED	
Michael Konick (HS student)	0.00	No
Alberto Almonte (HS student)	0.00	No
Bonlale Salaam (HS student)	0.00	No
FTE Equivalent:	**0.00**	
Total Number:	**3**	

Sub Contractors (DD882)

1 a. New Jersey Institute of Technology

1 b. University Heights

Newark NJ 07102-1982

Sub Contractor Numbers (c):

Patent Clause Number (d-1):

Patent Date (d-2):

Work Description (e):

Sub Contract Award Date (f-1): 4/19/2004 12:00:00AM

Sub Contract Est Completion Date(f-2): 4/18/2008 12:00:00AM

Inventions (DD882)

Scientific Progress

Scientific Progress Section of
Final Progress Report for
DESTRUCTION CHEMISTRY OF MUSTARD SIMULANTS

E. M. Fisher, F.C. Gouldin, J.W. Bozzelli

4/19/04-4/18/08

FUNDING NUMBER W911NF0410120
SCIENTIFIC PROGRESS AND ACCOMPLISHMENTS

ABSTRACT

This study investigates the destruction chemistry of organosulfur compounds under both pyrolytic and oxidative conditions. We focus on the destruction of alkyl sulfides that are surrogates for chemical warfare agents H, HD, and HT. We report our work on developing thermochemistry, reaction pathways and kinetic parameters for multiple chemical subsystems, using computational chemistry methods. We also report our experimental results from flow reactor experiments for pyrolysis and oxidation of two alkyl sulfides: diethyl sulfide and ethyl methyl sulfide. A detailed, elementary reaction, mechanism has been developed to describe the pyrolysis and oxidation chemistry relevant to these compounds.

TABLE OF CONTENTS

I. LIST OF TABLES

II. LIST OF FIGURES

Fig. 9a Major species (>10 ppm) for pyrolysis of ethyl methyl sulfide at 740 ºC (operating condition EP3). Hollow symbols represent FTIR data, while filled symbols represent GC/MS data.

Fig. 9b Minor species (<10 ppm) for pyrolysis of ethyl methyl sulfide at 740 ºC (operating condition EP3). Hollow symbols represent FTIR data, while filled symbols represent GC/MS data.

Fig. 10a Major species (>10 ppm) for oxidation of diethyl sulfide at 630 ºC with low O_2 loading (operating condition DO1). Lines represent calculations with mechanism version 2; symbols represent experiments. Hollow symbols represent FTIR data, while filled symbols represent GC/MS data.

Fig. 10b Minor species (<10 ppm) for oxidation of diethyl sulfide at 630 ºC with low O_2 loading (operating condition DO1). Lines represent calculations with mechanism version 2; symbols represent experiments. FTIR data only.

Fig. 11a Major species (>10 ppm) for oxidation of diethyl sulfide at 670 ºC with low O_2 loading (operating condition DO2). Lines represent calculations with mechanism version 2; symbols represent experiments. Hollow symbols represent FTIR data, while filled symbols represent GC/MS data.

Fig. 11b Minor species (<10 ppm) for oxidation of diethyl sulfide at 670 ºC with low O_2 loading (operating condition DO2). Lines represent calculations with mechanism version 2; symbols represent experiments. FTIR data only.

Fig. 12a Major species (>10 ppm) for oxidation of diethyl sulfide at 700 ºC with low O_2 loading (operating condition DO3). Lines represent calculations with mechanism version 2; symbols represent experiments. Hollow symbols represent FTIR data, while filled symbols represent GC/MS data.

Fig. 12b Minor species (<10 ppm) for oxidation of diethyl sulfide at 700 ºC with low O_2 loading (operating condition DO3). Lines represent calculations with mechanism version 2; symbols represent experiments. FTIR data only.

Fig. 13a Major species (>10 ppm) for oxidation of diethyl sulfide at 740 ºC with low O_2 loading (operating condition DO4). Lines represent calculations with mechanism version 2; symbols represent experiments. Hollow symbols represent FTIR data, while filled symbols represent GC/MS data.

Fig. 14a Major species (>10 ppm) for oxidation of diethyl sulfide at 700 ºC with high O_2 loading (operating condition DO5). Lines represent calculations with mechanism version 2; symbols represent experiments. Hollow symbols represent FTIR data, while filled symbols represent GC/MS data.

Fig. 14b Minor species (<10 ppm) for oxidation of diethyl sulfide at 700 ºC with high O_2 loading (operating condition DO5). Lines represent calculations with mechanism version 2; symbols represent experiments. FTIR data only.

Fig. 15a Major species (>10 ppm) for oxidation of diethyl sulfide at 740 ºC with medium O_2 loading (operating condition DO6). Lines represent calculations with mechanism version 2; symbols represent experiments. Hollow symbols represent FTIR data, while filled symbols represent GC/MS data.

Fig. 15b Minor species (<10 ppm) for oxidation of diethyl sulfide at 740 ºC with medium O_2 loading (operating condition DO6). Lines represent calculations with mechanism version 2; symbols represent experiments. FTIR data only.

Fig. 16a Major species (>10 ppm) for oxidation of diethyl sulfide at 740 ºC with high O_2 loading (operating condition DO7). Lines represent calculations with mechanism version 2; symbols represent experiments. Hollow symbols represent FTIR data, while filled symbols represent GC/MS data.

Fig. 16b Minor species (<10 ppm measured) for oxidation of diethyl sulfide at 740 ºC with high O_2 loading (operating condition DO7). Lines represent calculations with mechanism version 2; symbols represent experiments. FTIR data only.

Fig. 17a Major species (>10 ppm) for oxidation of ethyl methyl sulfide at 700 ºC with high O_2 loading (operating condition EO1). FTIR data only

Fig. 17b Minor species (<10 ppm) for oxidation of ethyl methyl sulfide at 700 ºC with high O_2 loading (operating condition EO1). FTIR data only

Fig. 18a Major species (>10 ppm) for oxidation of ethyl methyl sulfide at 740 ºC (operating condition EO2). FTIR data only.

Fig. 18b Minor species (<10 ppm) for oxidation of ethyl methyl sulfide at 740 ºC (operating condition EO2). FTIR data only.

Fig. 19 Element balances for diethyl sulfide pyrolysis data sets (operating conditions DP1, DP2, DP3, and DP4.)

Fig. 20 Major reaction pathways for diethyl sulfide pyrolysis. Dotted lines indicate radical attack reactions. Thicker lines represent reactions with larger rates.

Fig. 21 Major reaction pathways for diethyl sulfide oxidation. Dotted lines indicate radical attack reactions. Thicker lines represent reactions with larger rates.

III. PROBLEM STUDIED

We report the results of a study investigating the destruction chemistry of organosulfur compounds under pyrolytic and oxidative conditions. Sulfur compounds are common in combustion systems because of the presence of sulfur impurities in fuels such as coal and oil. However, the understanding of sulfur combustion chemistry is largely limited to the pathways leading to sulfur oxides. We address the early stages of destruction for alkyl sulfides, which are surrogates for the chemical warfare agents H, HD, and HT. We report computational chemistry and experimental flow reactor results contributing to the development and testing of a detailed chemical kinetic mechanism for the combustion and pyrolysis of diethyl sulfide. This mechanism can serve as a starting point for developing a mechanism for the related chemical warfare agents, which would be of value for predicting incinerator performance including off-design conditions. A similar effort with organophosphorus compounds has led to a detailed kinetic model of chemical warfare agent combustion, and its use in a model of an incinerator [1].

IV. IMPORTANT RESULTS

This section describes our major results. First we briefly summarize the computational chemistry methods and results for thermochemical properties, reaction pathways, and kinetic parameters. Then we discuss the two versions of the sulfide oxidation/pyrolysis mechanism developed during the project. Then we discuss the flow reactor experimental apparatus and method as well as the method for performing chemical kinetic simulations of the flow reactor experiments. Finally, experimental results and mechanism predictions are presented.

IV.A. Computational Chemistry and Mechanism Development Results

IV.A.1. Calculations of thermochemical properties

We have computed thermochemical properties for several classes of sulfur-containing species. The following method was used for the calculations: Isodesmic work reactions with various levels of theory have been used to calculate enthalpies of formation ($\Delta H_f^{o}{}_{298}$) of stable species and radicals. Entropy (S) and Heat capacity ($C_p(T)$) are determined using geometric parameters, vibrational frequencies and moments of inertia. Internal rotor potentials are calculated at the same level of theory.

Table 1 shows the classes of compounds for which thermochemical properties have been calculated, along with the theory level used. The thermochemical data resulting from these calculations are reported in our previous progress reports as well as in our publications and presentations. Thermochemical properties calculated as parts of the kinetic investigations described in the next section are not included in Table 1.

Table 1. Classes of compounds for which thermochemical properties have been obtained through computational chemistry.

Class of compounds	Example species	Level of theory
Sulfenic acids and esters and associated radicals	CH_3-S-OH, CH_3-S-OCH_3, CH_2·-S-OH	CBS-QB3, G3MP
Peroxy and hydroperoxy radicals associated with disulfide molecules	HSS-CH_2-OOH, CH_3-SS-CH_2-OOH, ·SS-CH_2-OOH, HSS-CH_2-OO·	B3LYP/6-31(d,p), CBS-QB3
Methyl sulfinic acid and ester and associated radicals	CH_3-S(=O)-OH, CH_3-S(=O)-OCH_3, CH_3-S(=O)-O·	B3LYP/6-31G(2d,p), B3LYP/6-31G(2d,dp), CBS-QB3
Ethenethiol and related radicals	CH2=CH-S-H, CH2=CH-S·	CBS-QB3, G3MP

IV.A.2. Calculations of reaction pathways and kinetics

For a number of reactions of interest in the hydrogen/carbon/sulfur/oxygen system, an initial reaction forms a chemically activated adduct to which numerous reaction pathways are available. This set of reaction pathways has been investigated computationally for a number of initial reactions, listed in Table 2.

Table 2. Multichannel reactions for which energy levels and/or kinetic parameters have been obtained through computational chemistry.

Initial reaction	Level of theory
HS•,+CO *CH_3S• +CO* *CH_3CH_2S• +CO* *CH_2=CH-CH_2S• +CO*	CBS-QB3 multilevel composite method for smaller radicals; density functional theory at B3LYP/6-31G(d.p) level.
CH_3SCH_2• + $^3O_2$	CBS-QB3 and B3LYP/6-311G(d,p))
CH_3S• + $^3O_2$	Multiple methods including B3LYP/6-311++G(d,p), B3LYP/6-311++G(3df,2p), CCSD(T)/6-311G(d,p) //MP2/6-31G(d,p), B3P86/6-311G(2d,2p)//B3P86/6-31G(d), and B3PW91/6-311++G (3df,2p). The CBS-QB3 and G3MP2 composite methods are recommended. G2 and G3 are also applied when necessary.
$CH_3S(=O)CH_2$• + $^3O_2$	CBS-QB3 and density functional theory
S=C•H+ $^3O_2$ *(oxidation of thioformyl radical)*	CBS-QB3, G3MP2, and G2 for enthalpies of reaction; B3LYP/6-311G(d,p) for S and Cp

The procedure for obtaining reaction pathways and kinetics is the following: First thermochemical properties are calculated for the adducts and the products of the reaction paths, as well as for the transition states for all reactions. The method for these calculations was similar to that described in the previous section. These results can be displayed in a diagram showing computed potential energy levels for each set of products or transition state. This potential energy level diagram can be interpreted qualitatively, to see which channels have relatively low barriers, and thus are likely to be most important. A representative energy level diagram is shown below, as Figure 1.

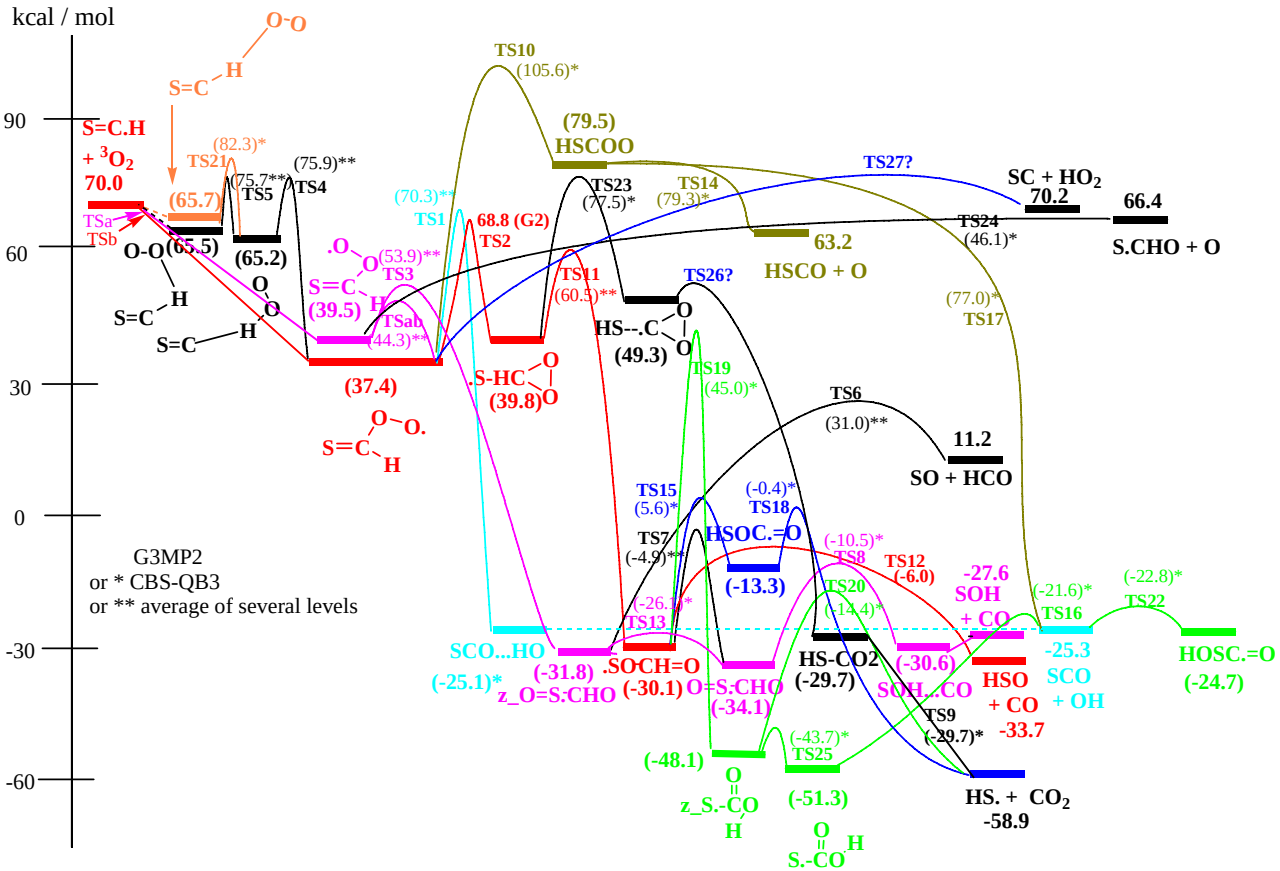

Figure 1: Potential Energy Diagram at 298 K (in kcal/mol) for the oxidation of the thioformyl radical. All barriers are calculated at G3MP2 level, except those labeled with * and **, which are calculated at CBS-QB3 and the average of several levels, respectively.

In the cases where more quantitative kinetic data was obtained, it was done so as follows: The rate constants for the elementary reactions were calculated from the computed frequencies, structures and energies using canonical transition state theory with rate constant values (T) fit to the three-parameter modified Arrhenius equation, $k = A \times T^n \times \exp(-Ea/RT)$. Temperature and pressure dependant rate constants were calculated with multi channel, multi frequency QRRK theory for $k(E)$ and Master equation analysis for fall-off [2]. A set of rate constants calculated from the energy levels shown in Figure 1 is shown below in Figure 2. Results of this analysis and others are presented in our reports and publications.

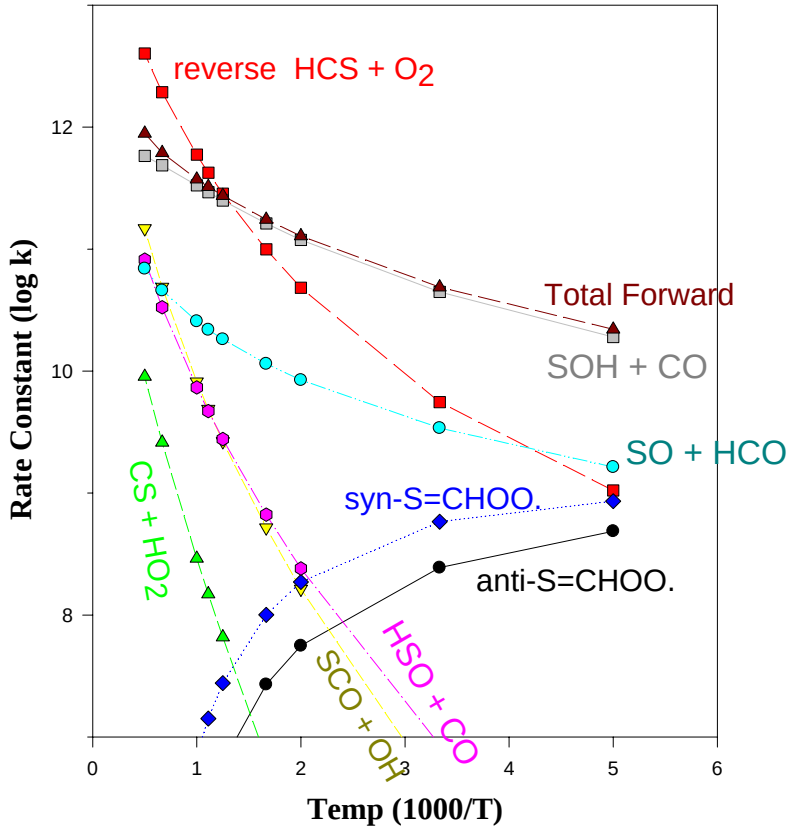

Figure 2: Calculated rate constants (log k) vs temperature (K) at 1 atm for reactions involved in the oxidation of the thiformyl radical.

IV.A.3. Development of a combustion chemistry mechanism for diethyl sulfide

A pyrolysis and oxidation mechanism has been developed for diethyl sulfide, along with species thermochemical parameters (enthalpy, entropy, and heat capacity) for molecule, radical intermediates, and transition state structures. The pyrolysis submechanism of Version 1 of the mechanism consists of 170 elementary reactions and 70 species that are components of approximately 25 chemical activation or multi-channel dissociation reaction systems. This submechanism is described in detail in Zheng et al.[3]. Version 2 is a similar mechanism with computational chemistry used at high levels to calculate rate constants on important reactions of the reacting sulfides and thiols. Version 2 includes rate constants determined at the CBS-QB3 and G3MP2 levels of theory for abstraction, elimination (beta scission from radical species and molecular elimination from both radicals and singlet molecules) and addition reactions related to the parent diethyl and dimethyl sulfides and ethyl and methyl thiols. Reactions for abstraction and elimination of hydrogen atoms from the sulfide and thiol moieties include tunneling corrections using the Wigner method, plus degeneracy and symmetry contributions.

IV.B. Experimental Results and Comparison of Mechanisms to Experiments

IV.B.1. Experimental method

We have used a turbulent flow reactor with extractive sampling to examine the destruction of two mustard simulants under both pyrolytic and oxidative conditions. The flow reactor is shown in Fig. 3 and is described briefly here; more details are given in a recent publication [3]. The flow reactor consisted of a main flow and a secondary flow. Nitrogen was metered and passed through a retort inside a furnace. The main flow went through a heated flow development section, followed by an injection section in which the secondary flow (simulant + N_2 and O_2 or CO) was added via four turbulent jets. Next came the reaction section, a quartz tube with 45 mm ID, 48 mm OD, and 100 cm length, held inside a larger heated stainless steel pipe. Four ports on the stainless steel pipe were aligned with the holes in the quartz tube, allowing the insertion of probes for centerline gas sampling. Temperatures measured along the flow reactor axis are shown in Fig. 4.

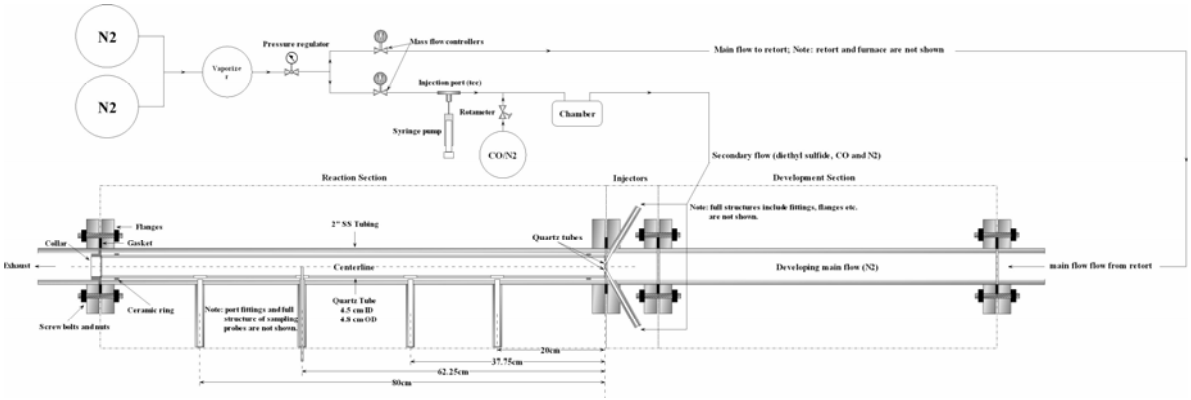

Figure 3. Schematic of Flow Reactor

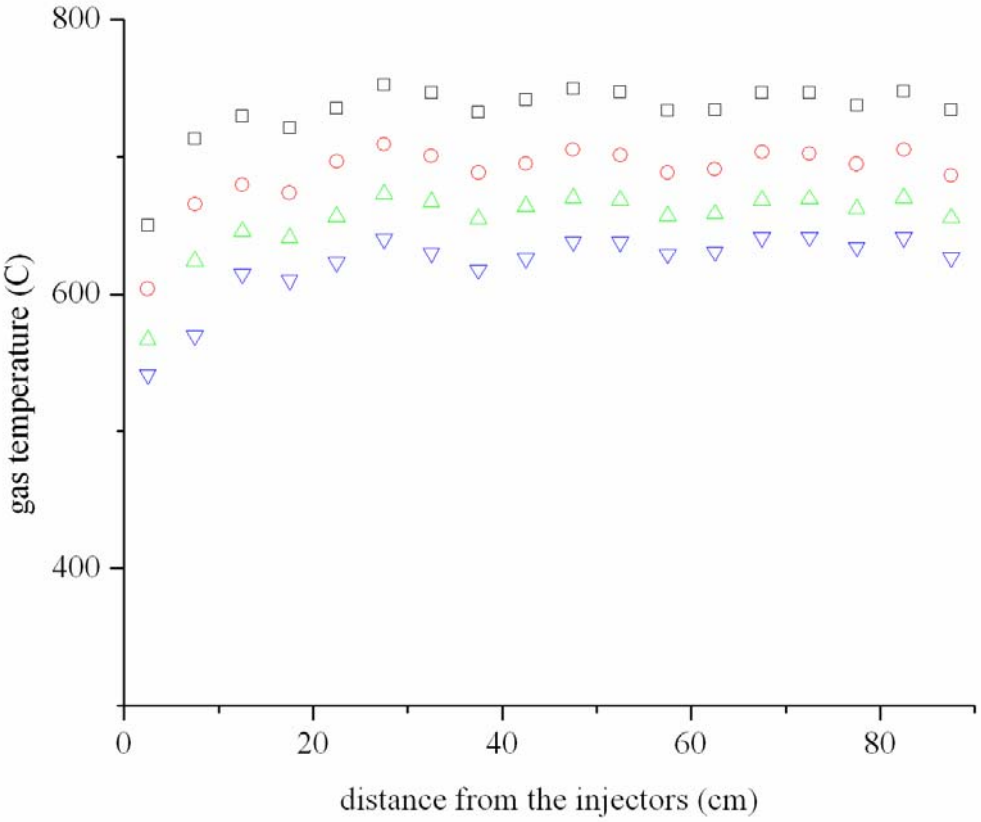

Figure 4. Reaction section axial temperature profiles. The four different symbols represent different operating conditions with nominal temperatures of 630, 670, 700, and 740 C. Lower temperatures occur at short distances from the injectors as the cooler secondary flow mixes into the main flow.

Samples were withdrawn from the reactor via a quartz probe. In order to quench reactions, the sample flow was diluted to approximately 50% of its original concentration with a flow of nitrogen inside the quartz probe. A simple adiabatic mixing calculation indicates that the dilution should cool the sample flow to temperatures at which no composition changes in the product stream are predicted to occur. Downstream of the probe, the diluted sample was drawn through Teflon® (Dupont) tubing either into the long-path gas cell of a FTIR (Nicolet 6700) or into the gas sampling loop of a GC/MS (Thermo Focus GC/DSQII MS) for sample analysis. For details of the sampling and analysis methods, see Zheng et al. [3]. The FTIR was used mainly for light hydrocarbons, while the GC/MS yielded information about the parent compound as well as minor sulfur-containing products. Typical sensitivities of the two instruments range from 50 ppb to 1.5 ppm.

The sample species concentrations depend on the sample dilution and on the rate of mixing of main and secondary flows, as well as on the rates of chemical reactions occurring in the flow reactor. For the pyrolysis experiments, CO was shown to be inert, and was used as a tracer to adjust the measured species concentrations to account for

mixing and dilution. The measured mole fraction CO versus distance is shown in Fig. 3 for the different temperature conditions. For the oxidation experiments, CO was not a viable tracer, as it could react with oxygen. The mixing/dilution information obtained from CO tracer during the pyrolysis experiments was consistent from run to run, and was applied to the oxidation data sets.

IV.B.2. Computational method

The flow reactor was simulated as a plug flow reactor in CHEMKIN [4], with centerline measured temperatures as inputs to the calculation, and with no wall reactions. Experiments were performed with either diethyl sulfide or ethyl methyl sulfide as the parent compound. (See operating conditions below.) Only the diethyl sulfide experiments were simulated, as the kinetic mechanism did not include the initial stages of the decomposition of ethyl methyl sulfide. Two different kinetic mechanisms are used, as described in Section IV.A.3 above. Mechanism Version 1, described in a previous publication [2], was used to simulate the diethyl sulfide pyrolysis experiments. Mechanism Version 2, which differs from Mechanism Version 1 only through the use of a higher level of theory in the calculation of some rate constants and thermochemical parameters, was used to simulate the diethyl sulfide oxidation experiments.

IV.B.3. Operating conditions

Tables 3 through 6 show the flow reactor operating conditions for the four experimental data sets obtained (total of 12 operating conditions with two different chemical warfare agent simulants). These data sets are: pyrolysis of diethyl sulfide (Table 3) and of ethyl methyl sulfide (Table 4), and oxidation of diethyl sulfide (Table 5) and of ethyl methyl sulfide (Table 6). The temperature profiles are as shown in Figure 4. In tables 5 and 6, the equivalence ratio is based on the conversion of sulfur to SO_2, carbon to CO_2, and hydrogen to H_2O for complete combustion

Table 3. Flow reactor operating conditions for diethyl sulfide pyrolysis experiments. In these experiments the secondary flow consisted of N_2, CO, and diethyl sulfide.

Condition	Nominal Temperature (ºC)	Flowrate of Main N_2 flow (slpm)	Flowrate of Secondary N_2 flow (slpm)	Well-mixed CO loading in reaction section (ppm)	Well-mixed initial diethyl sulfide loading (ppm)	Reynolds number
DP1	630	330	14.1	68.6	150	5022
DP2	670	341	15.3	66.3	150	5022
DP3	700	347	16.0	65.1	150	5022
DP4	740	350	16.8	64.4	150	5022

Table 4. Flow reactor operating conditions for ethyl methyl sulfide pyrolysis experiments. In these experiments the secondary flow consisted of N_2, CO, and ethyl methyl sulfide.

Condition	Nominal Temperature (ºC)	Flowrate of Main N_2 flow (slpm)	Flowrate of Secondary N_2 flow (slpm)	Well-mixed CO loading in reaction section (ppm)	Well-mixed initial ethyl methyl sulfide loading (ppm)	Reynolds number
EP1	630	330	14.1	68.6	150	5020
EP2	700	347	16.0	65.1	150	5060
EP3	740	350	16.8	64.4	150	4990

Table 5. Flow reactor operating conditions for diethyl sulfide oxidation experiments. In these experiments the secondary flow consisted of N_2, O_2, and diethyl sulfide.

Condition	Nominal Temperature (ºC)	Flowrate of Main N_2 flow (slpm)	Flowrate of Secondary N_2 flow (slpm)	Well-mixed initial O_2 loading in reaction section (ppm)	Well-mixed initial diethyl sulfide loading (ppm)	Equivalence Ratio	Reynolds number
DO1	630	330	13.3	733	100	1.02	5020
DO2	670	341	14.4	708	100	1.06	5060
DO3	700	347	15.2	695	100	1.08	5060
DO4	740	350	16.0	687	100	1.09	4990
DO5	700	347	16.4	9042	100	0.083	5060
DO6	740	350	13.7	1960	100	0.383	4990
DO7	740	350	17.3	9415	100	0.080	4990

Table 6. Flow reactor operating conditions for ethyl methyl sulfide oxidation experiments. In these experiments the secondary flow consisted of N_2, O_2, and ethyl methyl sulfide.

Condition	Nominal Temperature (ºC)	Flowrate of Main N_2 flow (slpm)	Flowrate of Secondary N_2 flow (slpm)	Well-mixed initial O_2 loading in reaction section (ppm)	Well-mixed initial ethyl methyl sulfide loading (ppm)	Equivalence Ratio	Reynolds number
EO1	700	347	16.4	9042	150	0.124	5060
EO2	740	350	17.3	9415	150	0.119	4990

IV.B.4. Results: species profiles

Figures 5 through 18 show experimental and calculated species profiles for the conditions described in the previous section. Sampling locations have been converted to residence times using the bulk velocity. As mentioned above, calculations were performed only for

the diethyl sulfide runs, and make use of two different versions of the mechanism. Version 1 is used in the pyrolysis simulations, and version 2 is used in the oxidation simulations. Lines represent calculations, while symbols represent experimental results, mainly with FTIR. As can be seen from the figures, most experimental data points were measured twice, with good repeatability. In some cases, both GC/MS and FTIR measurement results are available and are represented by different symbols. Agreement between the two methods is good in these cases. Included in these figures are experimental and computational profiles for all species experimentally measured at levels above 1 ppm.

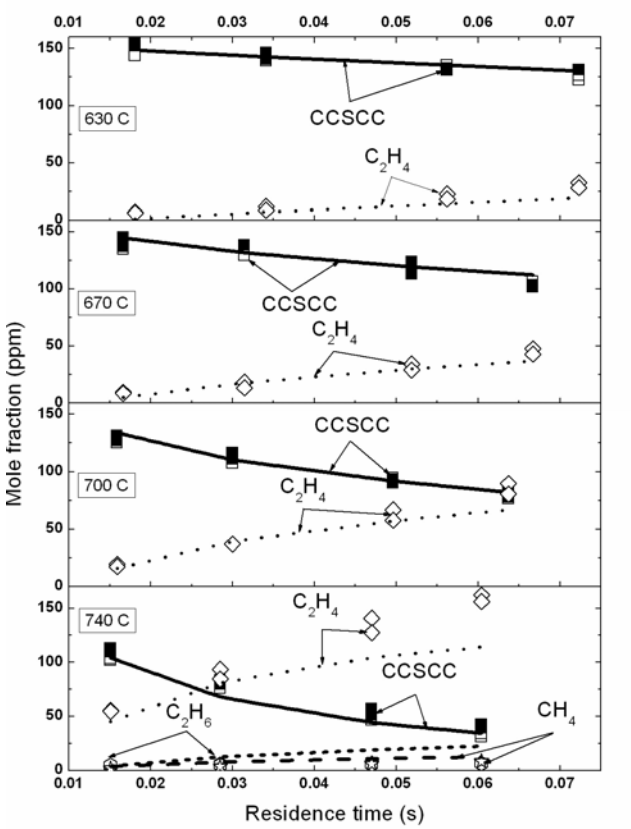

Fig. 5. Major species (>10 ppm) in pyrolysis of diethyl sulfide. Lines represent calculations with mechanism version 1; symbols represent experiments. Hollow symbols represent FTIR data, while filled symbols represent GC/MS data. Operating conditions DP1, DP2, DP3, and DP4.

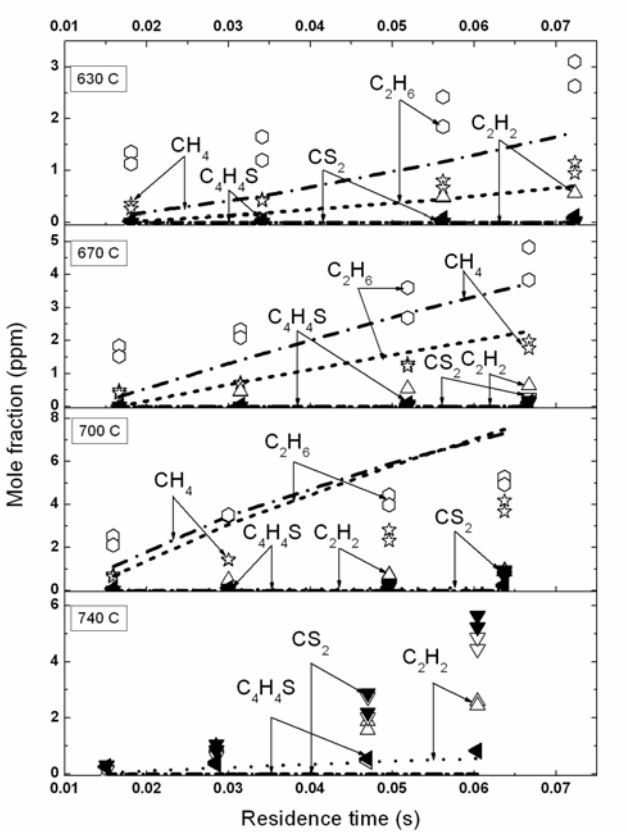

Fig. 6. Minor species (<10 ppm) in pyrolysis of diethyl sulfide. Lines represent calculations with mechanism version 1; symbols represent experiments. Hollow symbols represent FTIR data, while filled symbols represent GC/MS data. Operating conditions DP1, DP2, DP3, and DP4.

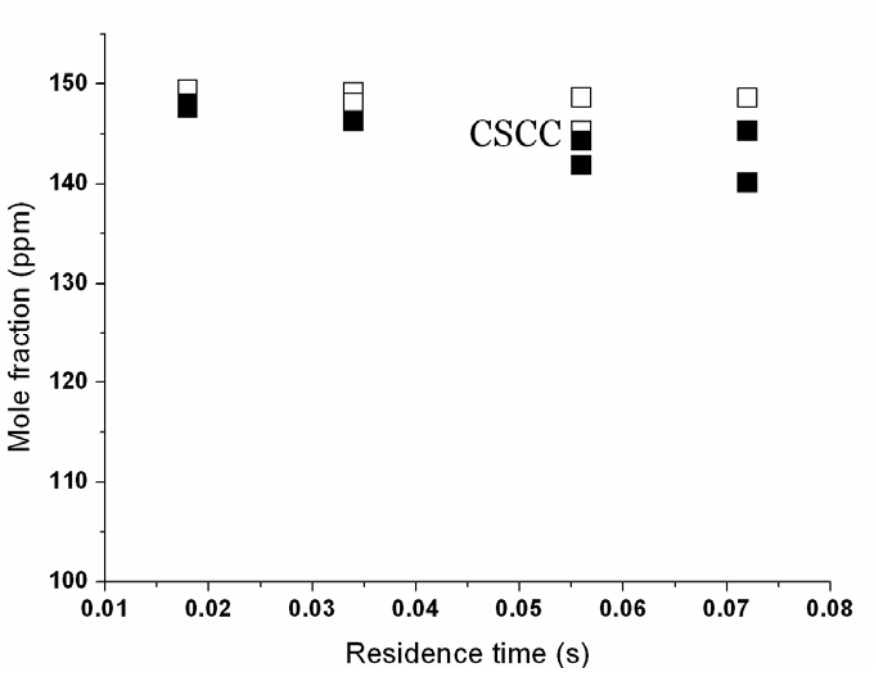

Fig. 7a Major species (>10 ppm) for pyrolysis of ethyl methyl sulfide at 630 ºC (operating condition EP1). Hollow symbols represent FTIR data, while filled symbols represent GC/MS data.

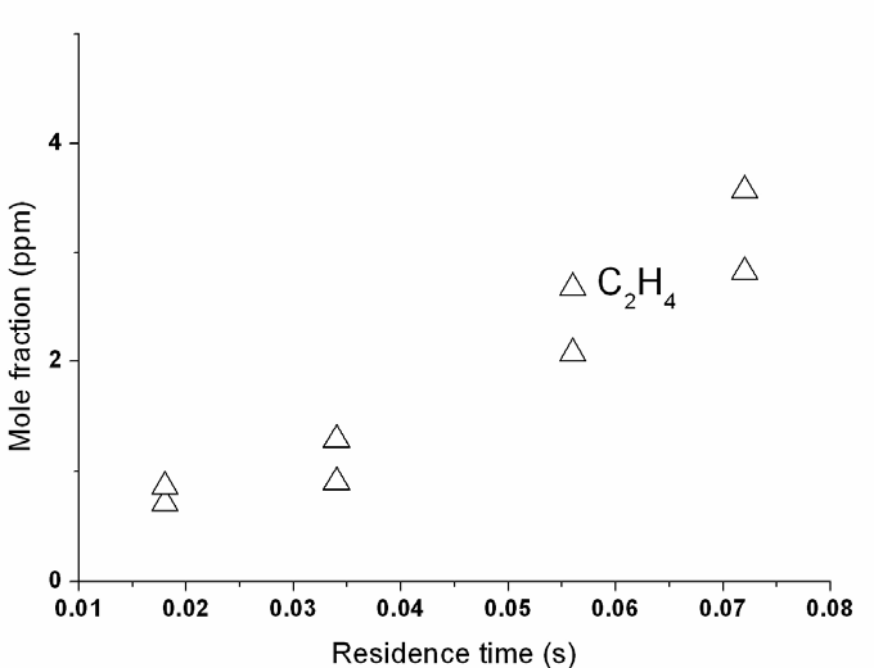

Fig. 7b Minor species (<10 ppm) for pyrolysis of ethyl methyl sulfide at 630 ºC (operating condition EP1). FTIR data only.

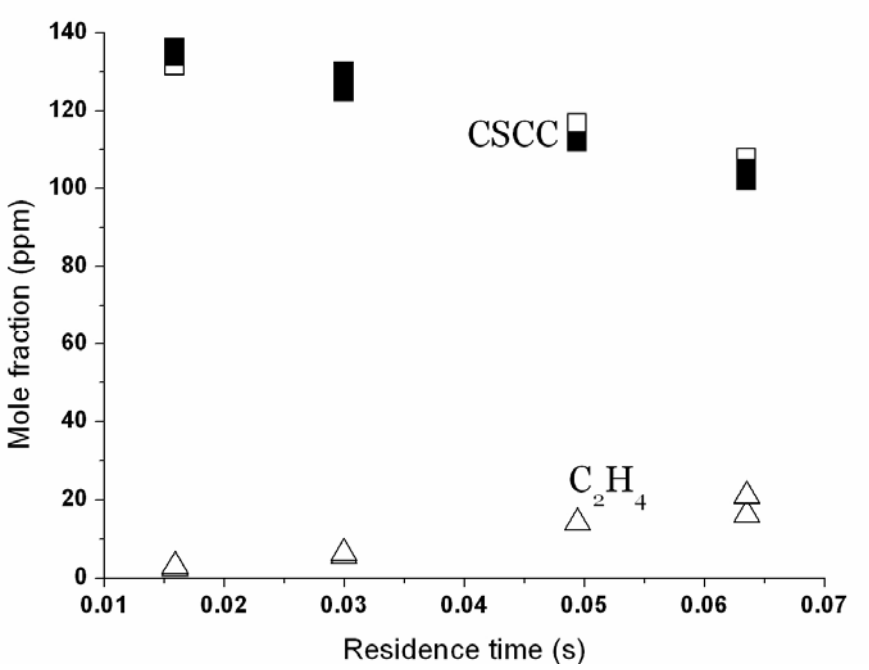

Fig. 8a Major species (>10 ppm) for pyrolysis of ethyl methyl sulfide at 700 ºC (operating condition EP2). Hollow symbols represent FTIR data, while filled symbols represent GC/MS data.

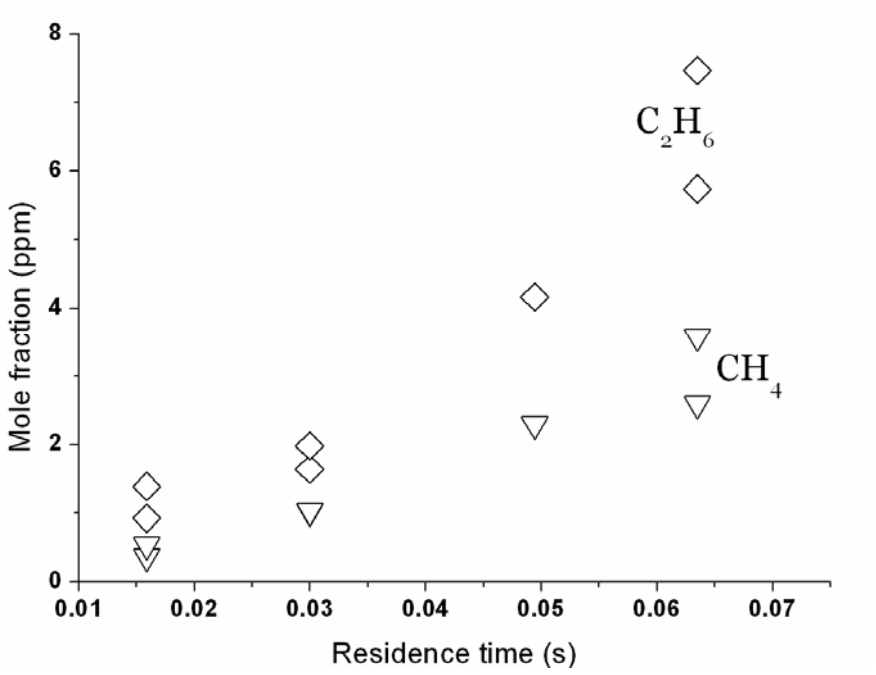

Fig. 8b Minor species (<10 ppm) for pyrolysis of ethyl methyl sulfide at 700 ºC (operating condition EP2). FTIR data only.

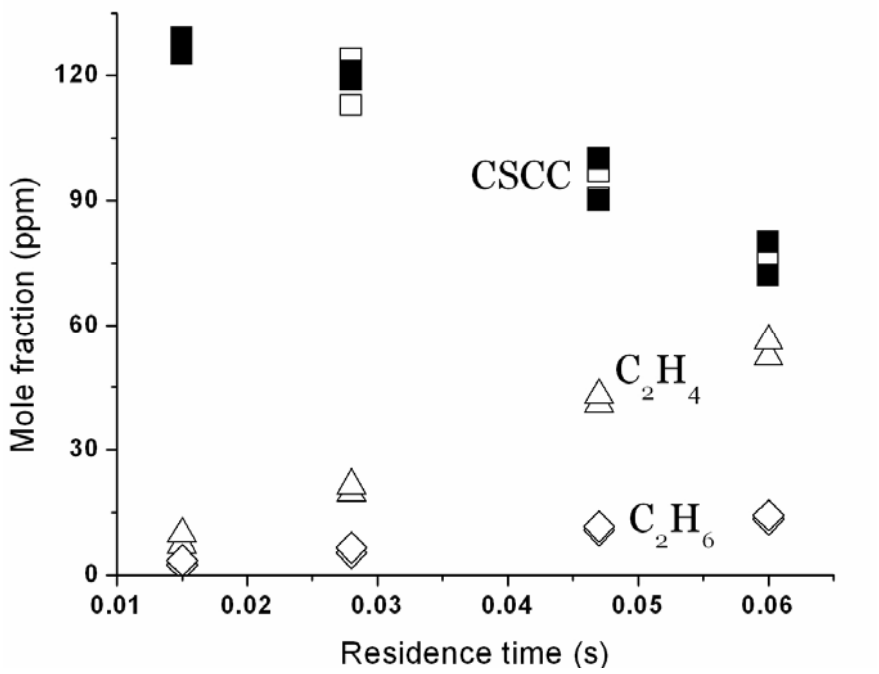

Fig. 9a Major species (>10 ppm) for pyrolysis of ethyl methyl sulfide at 740 ºC (operating condition EP3). Hollow symbols represent FTIR data, while filled symbols represent GC/MS data.

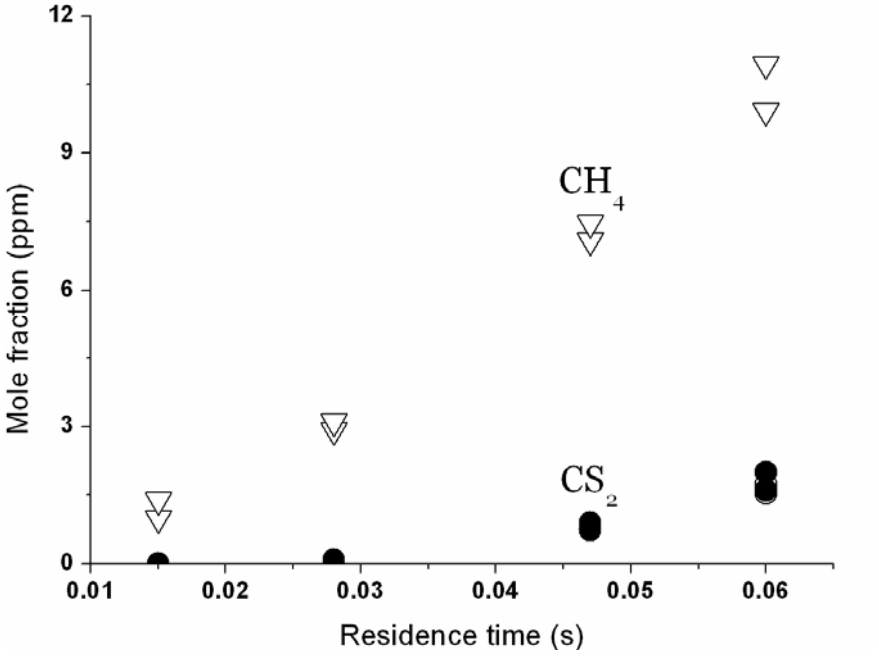

Fig. 9b Minor species (<10 ppm) for pyrolysis of ethyl methyl sulfide at 740 ºC (operating condition EP3). Hollow symbols represent FTIR data, while filled symbols represent GC/MS data.

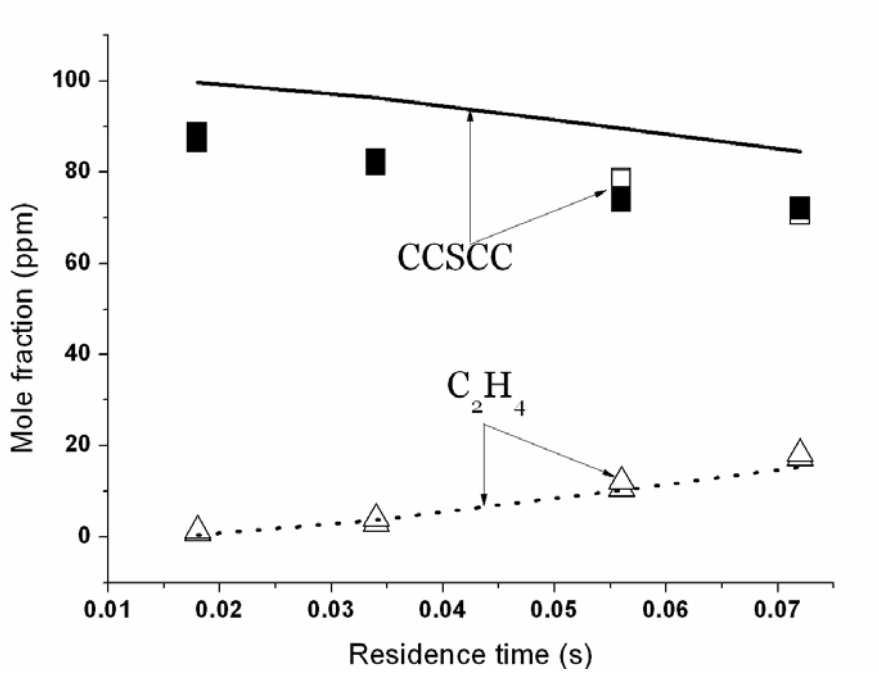

Fig. 10a Major species (>10 ppm) for oxidation of diethyl sulfide at 630 ºC with low O_2 loading (operating condition DO1). Lines represent calculations with mechanism version 2; symbols represent experiments. Hollow symbols represent FTIR data, while filled symbols represent GC/MS data.

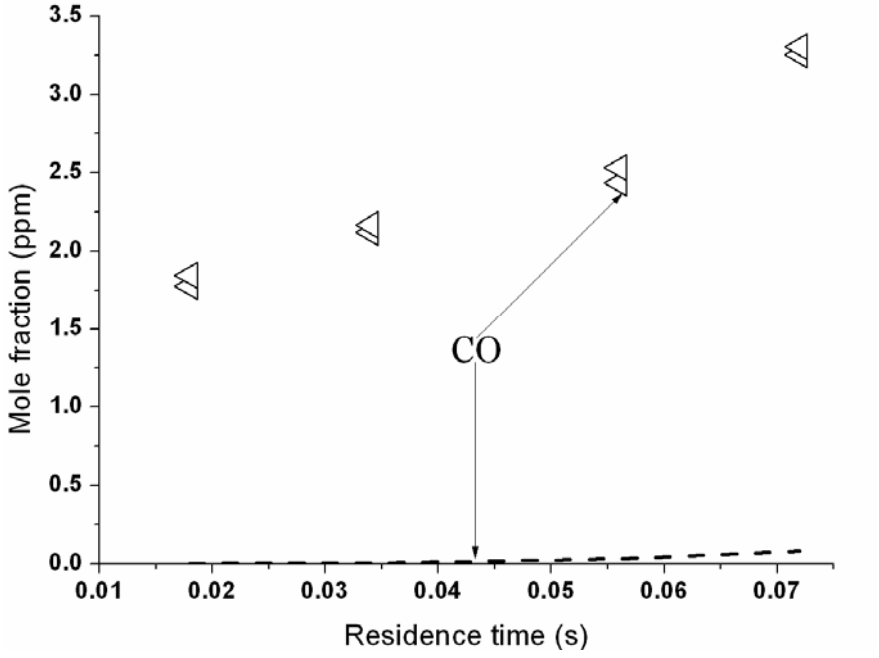

Fig. 10b Minor species (<10 ppm) for oxidation of diethyl sulfide at 630 ºC with low O_2 loading (operating condition DO1). Lines represent calculations with mechanism version 2; symbols represent experiments. FTIR data only.

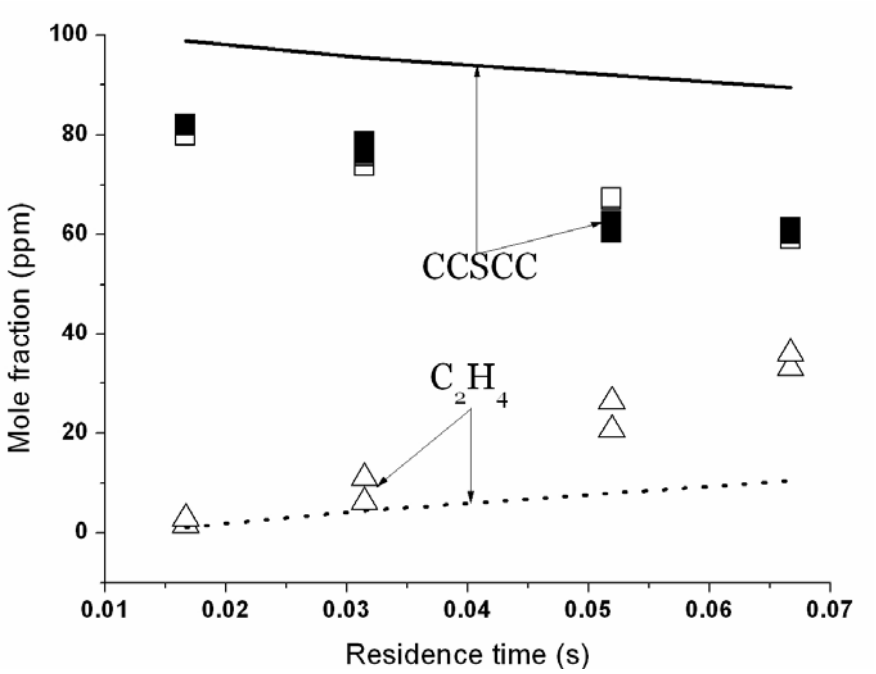

Fig. 11a Major species (>10 ppm) for oxidation of diethyl sulfide at 670 ºC with low O_2 loading (operating condition DO2). Lines represent calculations with mechanism version 2; symbols represent experiments. Hollow symbols represent FTIR data, while filled symbols represent GC/MS data.

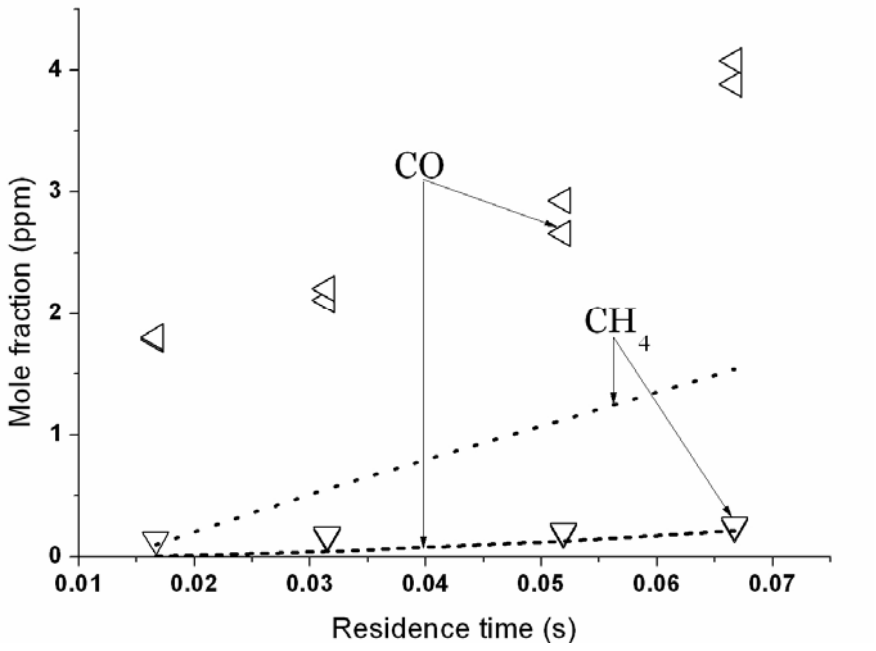

Fig. 11b Minor species (<10 ppm) for oxidation of diethyl sulfide at 670 ºC with low O_2 loading (operating condition DO2). Lines represent calculations with mechanism version 2; symbols represent experiments. FTIR data only.

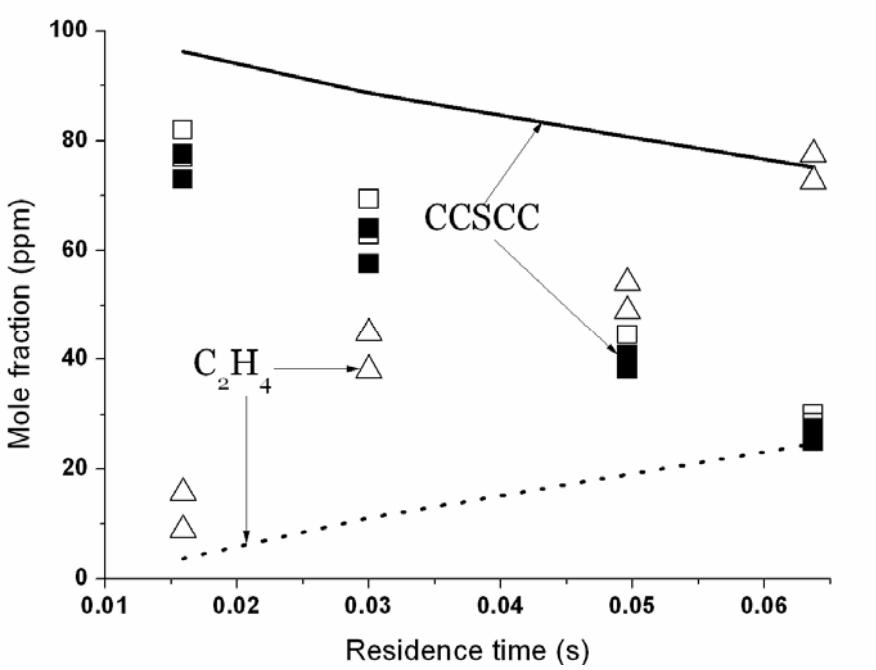

Fig. 12a Major species (>10 ppm) for oxidation of diethyl sulfide at 700 ºC with low O_2 loading (operating condition DO3). Lines represent calculations with mechanism version 2; symbols represent experiments. Hollow symbols represent FTIR data, while filled symbols represent GC/MS data.

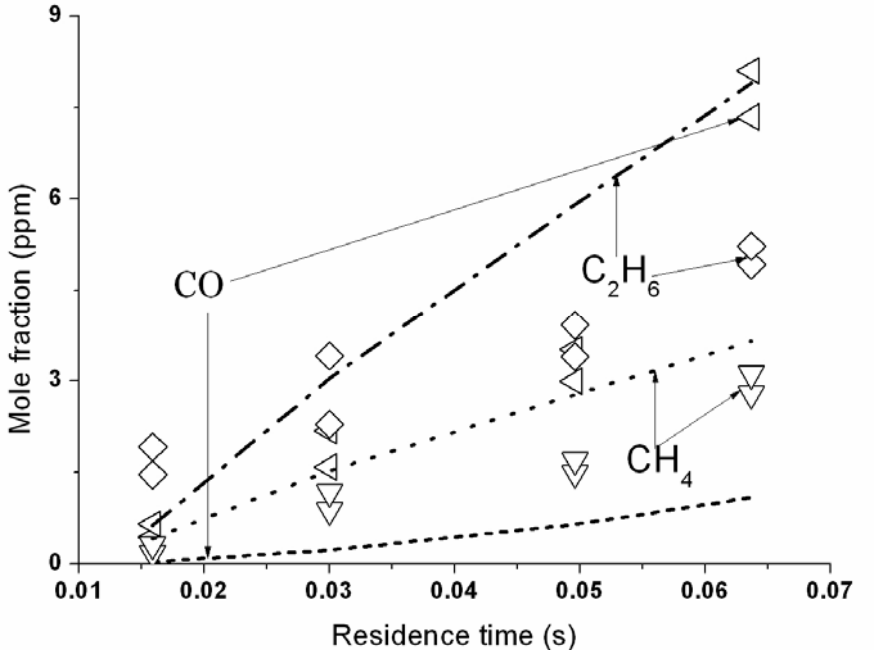

Fig. 12b Minor species (<10 ppm) for oxidation of diethyl sulfide at 700 ºC with low O_2 loading (operating condition DO3). Lines represent calculations with mechanism version 2; symbols represent experiments. FTIR data only.

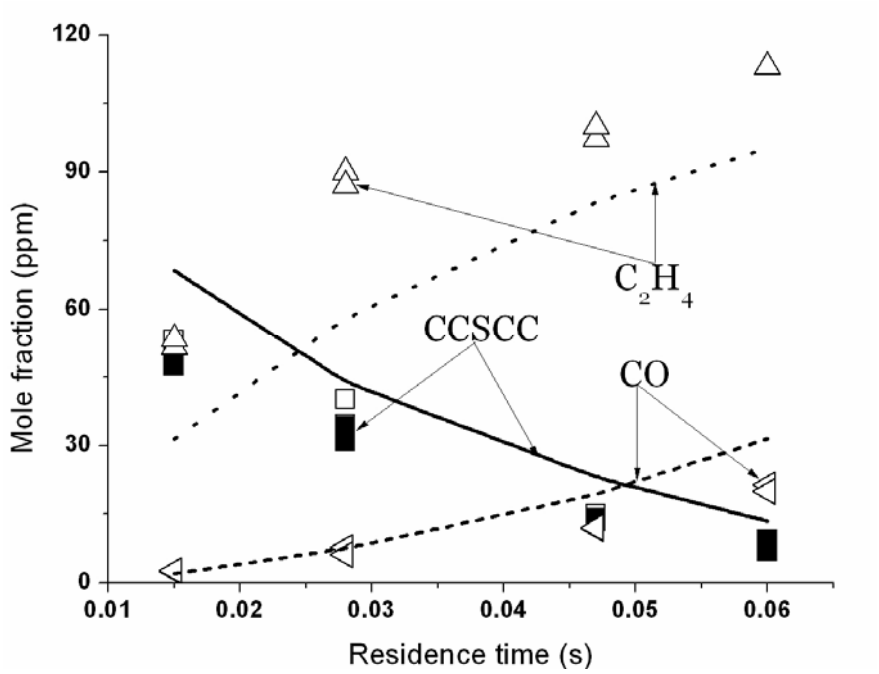

Fig. 13a Major species (>10 ppm) for oxidation of diethyl sulfide at 740 ºC with low O_2 loading (operating condition DO4). Lines represent calculations with mechanism version 2; symbols represent experiments. Hollow symbols represent FTIR data, while filled symbols represent GC/MS data.

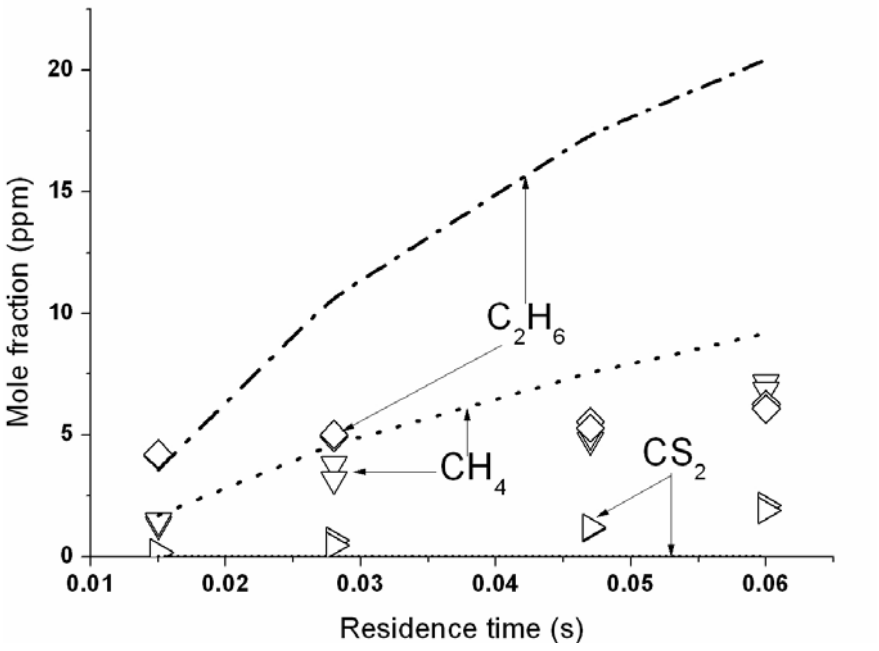

Fig. 13b Minor species (<10 ppm) for oxidation of diethyl sulfide at 740 ºC with low O_2 loading (operating condition DO4). Lines represent calculations with mechanism version 2; symbols represent experiments. FTIR data only.

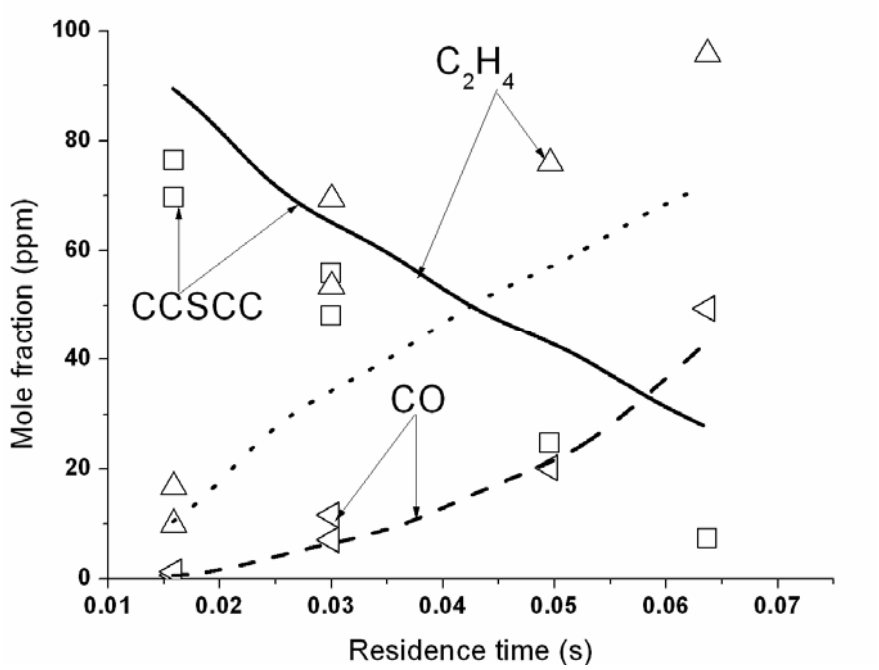

Fig. 14a Major species (>10 ppm) for oxidation of diethyl sulfide at 700 ºC with high O_2 loading (operating condition DO5). Lines represent calculations with mechanism version 2; symbols represent experiments. Hollow symbols represent FTIR data, while filled symbols represent GC/MS data.

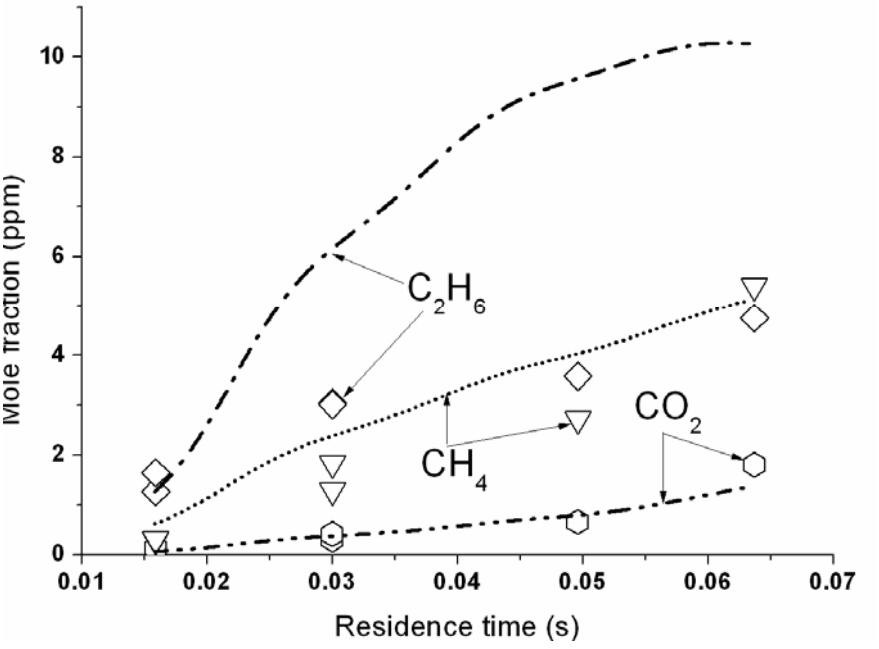

Fig. 14b Minor species (<10 ppm) for oxidation of diethyl sulfide at 700 ºC with high O_2 loading (operating condition DO5). Lines represent calculations with mechanism version 2; symbols represent experiments. FTIR data only.

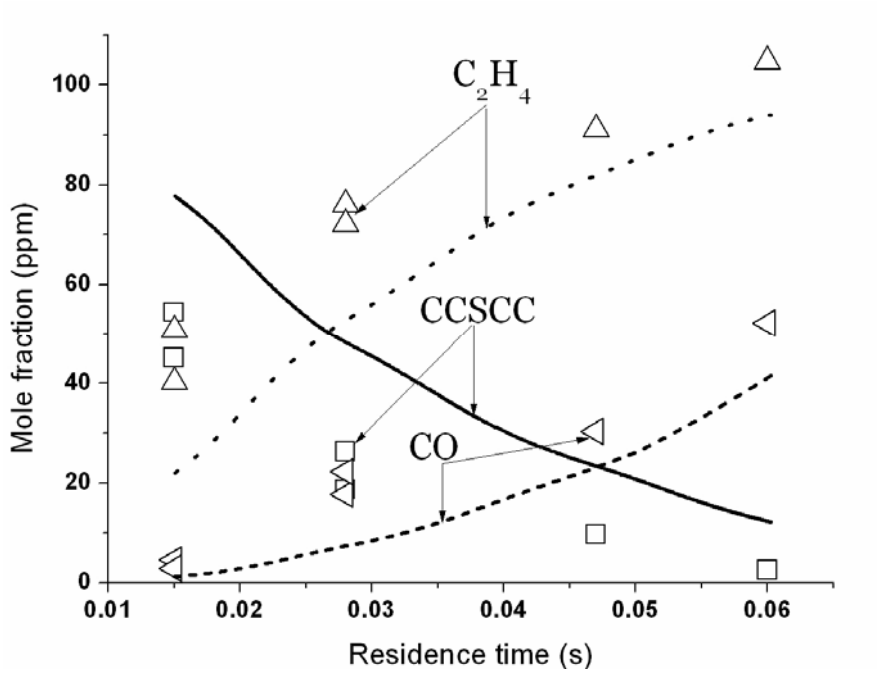

Fig. 15a Major species (>10 ppm) for oxidation of diethyl sulfide at 740 ºC with medium O_2 loading (operating condition DO6). Lines represent calculations with mechanism version 2; symbols represent experiments. Hollow symbols represent FTIR data, while filled symbols represent GC/MS data.

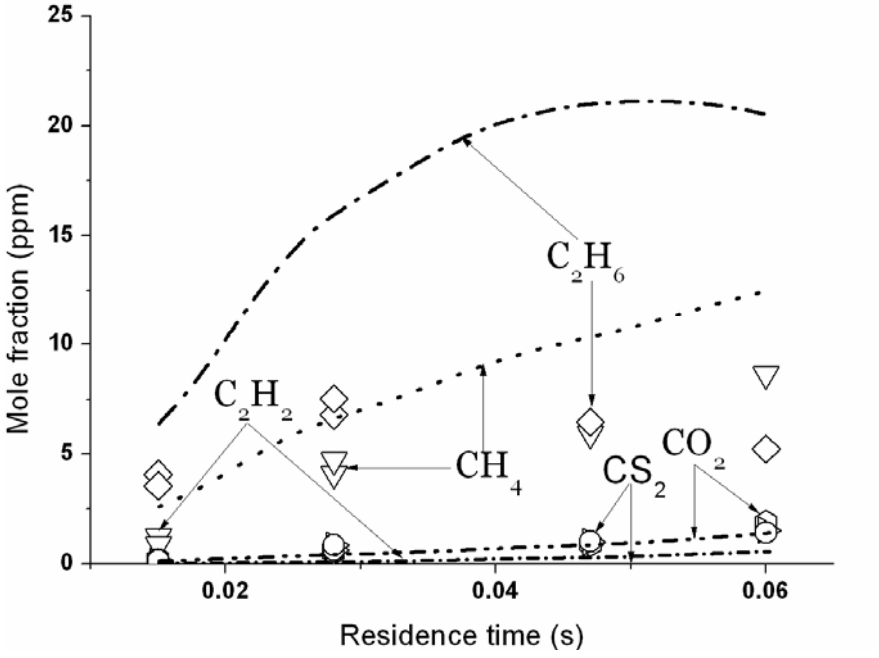

Fig. 15b Minor species (<10 ppm) for oxidation of diethyl sulfide at 740 ºC with medium O_2 loading (operating condition DO6). Lines represent calculations with mechanism version 2; symbols represent experiments. FTIR data only.

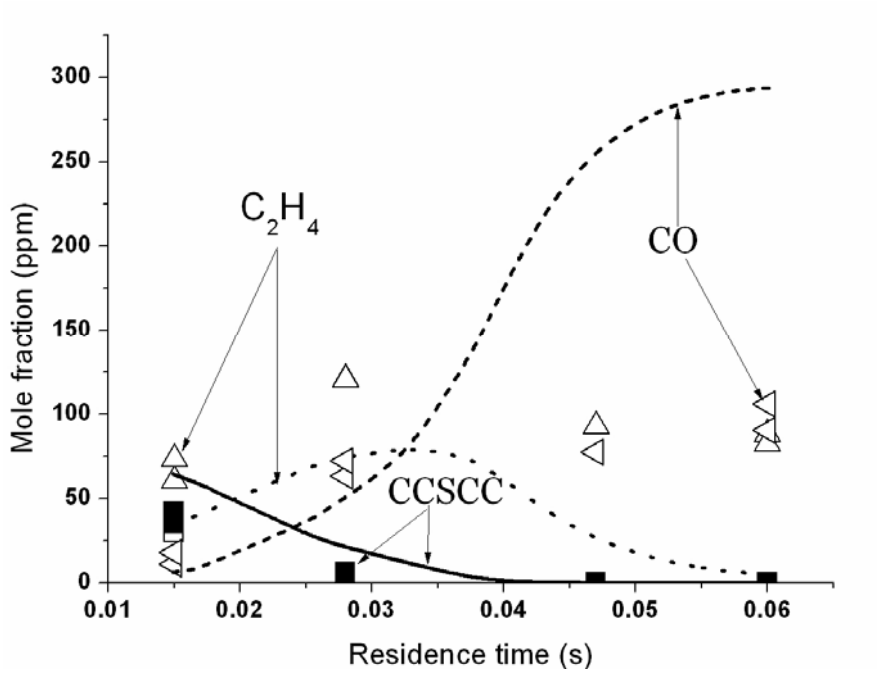

Fig. 16a Major species (>10 ppm) for oxidation of diethyl sulfide at 740 ºC with high O_2 loading (operating condition DO7). Lines represent calculations with mechanism version 2; symbols represent experiments. Hollow symbols represent FTIR data, while filled symbols represent GC/MS data.

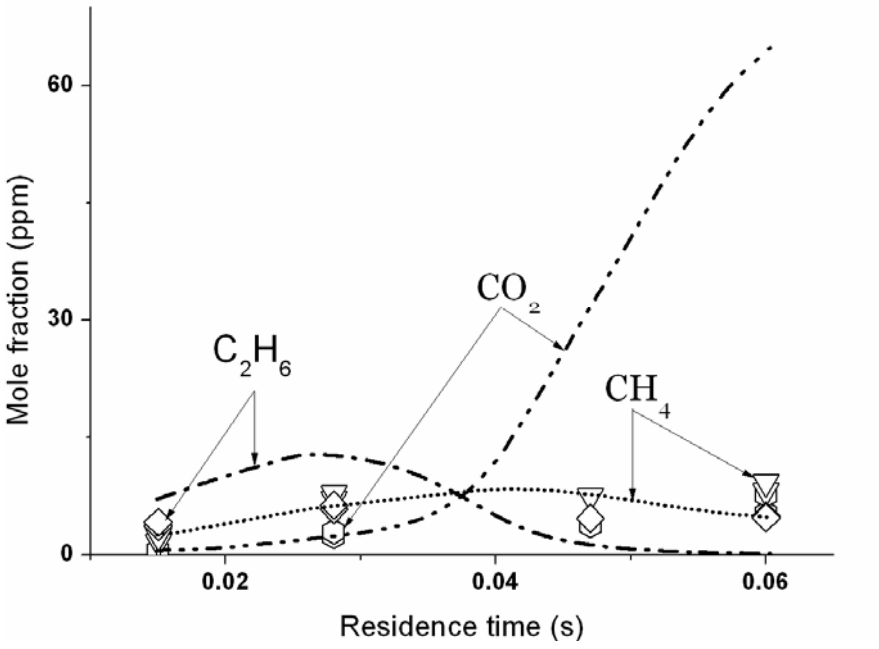

Fig. 16b Minor species (<10 ppm measured) for oxidation of diethyl sulfide at 740 ºC with high O_2 loading (operating condition DO7). Lines represent calculations with mechanism version 2; symbols represent experiments. FTIR data only.

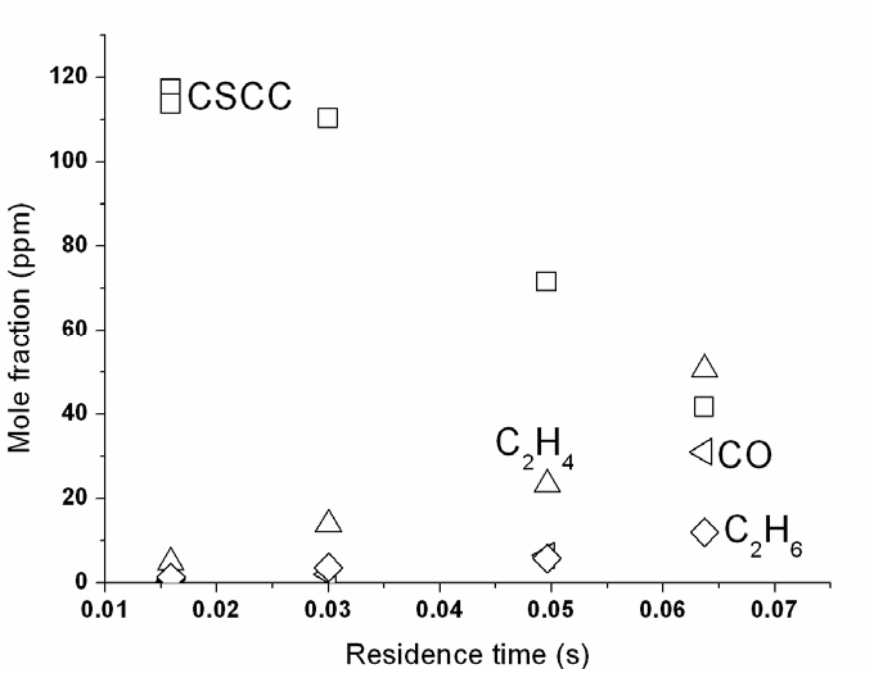

Fig. 17a Major species (>10 ppm) for oxidation of ethyl methyl sulfide at 700 ºC with high O_2 loading (operating condition EO1). FTIR data only

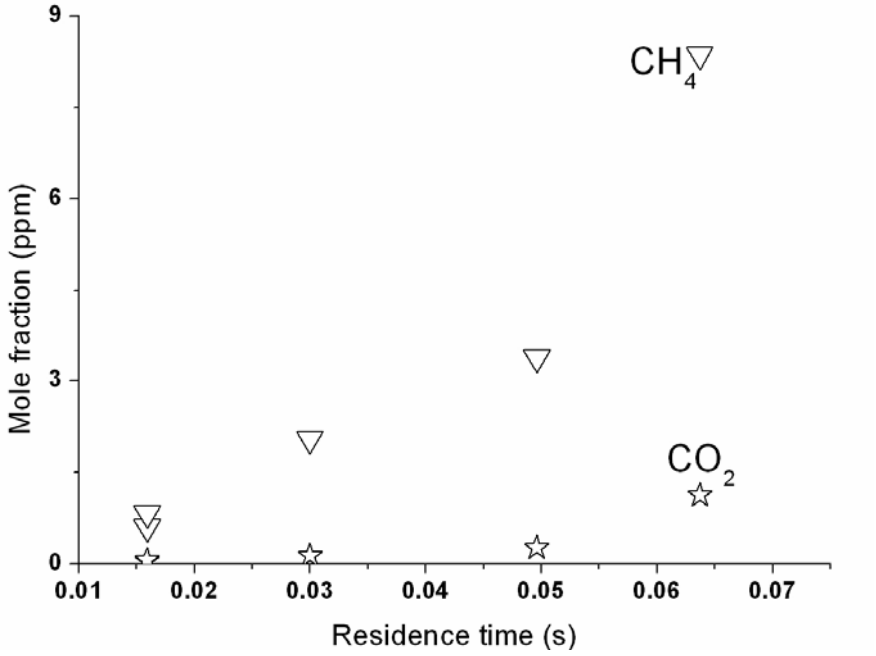

Fig. 17b Minor species (<10 ppm) for oxidation of ethyl methyl sulfide at 700 ºC with high O_2 loading (operating condition EO1). FTIR data only

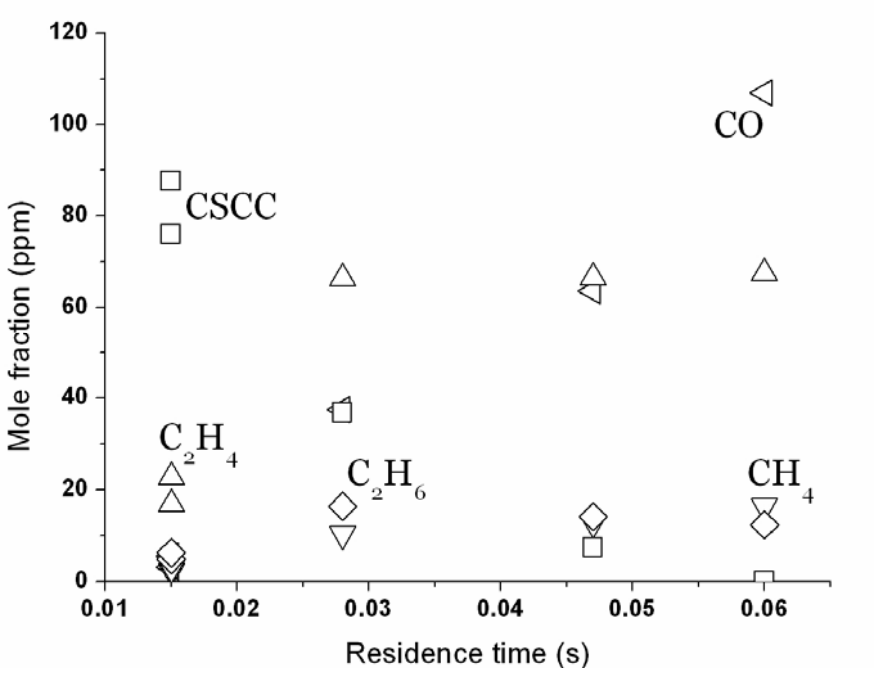

Fig. 18a Major species (>10 ppm) for oxidation of ethyl methyl sulfide at 740 ºC (operating condition EO2). FTIR data only.

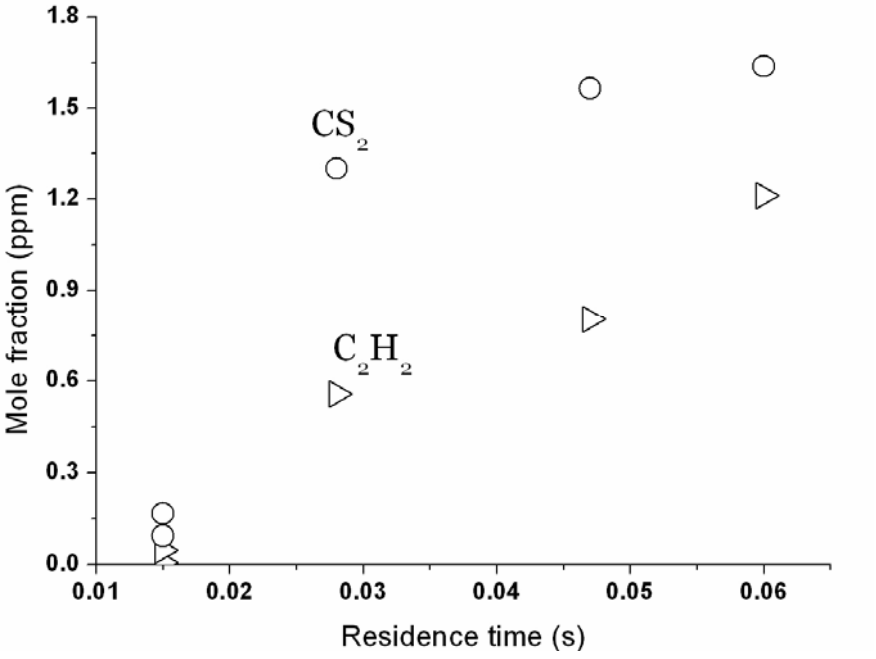

Fig. 18b Minor species (<10 ppm) for oxidation of ethyl methyl sulfide at 740 ºC (operating condition EO2). FTIR data only.

IV.B.5. Results: other species

Sulfur balances obtained from experimentally measured mole fractions were poor; carbon and hydrogen balances were better, but nonetheless imply the presence significant undetected species. Figure 19 shows the element balances for the diethyl sulfide pyrolysis data set as functions of destruction efficiency; other data sets gave similar results.

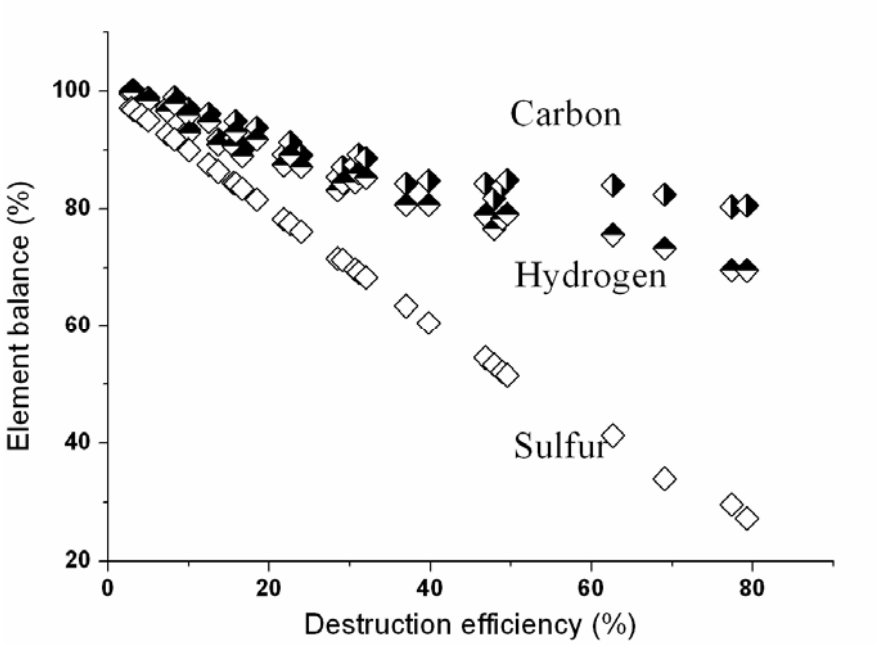

Fig. 19 Element balances for diethyl sulfide pyrolysis data sets (operating conditions DP1, DP2, DP3, and DP4.)

The most likely cause of the element balances is the presence of major species that are either undetectable or unable to pass through the sampling system. The kinetics calculations indicate the presence of three major species that are not detected: hydrogen (H_2), thioformaldehyde (CH_2=S), and thioacetaldehyde (CH_3CH=S). Of these, hydrogen is not detectable by either FTIR or GC/MS with the current analytical method. The two thioaldehydes, on the other hand, should be detectable by FTIR at the levels predicted. The absence of their spectral features in the FTIR absorption spectra suggests that they are lost in the sampling system. One possibility was that trimers would form from these compounds [5] and would not be volatile enough to travel through the sampling system; this possibility was investigated as described in the following paragraph.

In addition, a number of species were observed experimentally, by GC/MS, but not quantified. Of these, SO_2 appears to be present in significant quantities in the oxidation runs and we have plans to quantify it. Other species, for example: ethanethiol, methyl thiirane, ethyl methyl disulfide, and diethyl disulfide, are estimated to be present at levels below 1 ppm and do not have a significant impact on the element balances.

Light yellow condensates were observed in the sampling probes in the pyrolysis experiments, and their composition was investigated as follows: Methylene chloride

(CH_2Cl_2) was used to rinse these sampling probes, and part of the light yellow condensate was dissolved in the solvent. GC/MS analysis was performed with a J&W DB5 column. Although the rinsing and analysis method was able to detect thioaldehyde trimer from a purchased sample, no such trimer was detected in the sample from the probes. Instead a cyclic elemental sulfur compound, S_8, was identified in the rinsate. Thus the analysis of the rinsate provided no direct evidence of the thioaldehydes predicted by the kinetic calculations. Clearly, the presence of sulfur in the wall deposits helps to explain the poor sulfur balance, but the magnitude of the contribution is unknown, as is the route by which the cyclic sulfur compound is formed.

IV.B.6. Comparison between calculations and experiment

Two different versions of the kinetic mechanism were compared to predictions. Version 1 was used for the diethyl sulfide pyrolysis calculations, and this version was successful in predicting diethyl sulfide destruction. The only major product observed experimentally was ethylene, which appears at roughly the rate that the diethyl sulfide disappears. The calculations underpredict observed ethylene levels by approximately 30%. Among the product species observed and predicted, methane is overpredicted by approximately 50 to 100%. Carbon disulfide, thiophene, and acetylene are underpredicted. Ethane is underpredicted at low temperatures, but overpredicted at high temperatures.

Version 2 of the kinetic mechanism was used for the diethyl sulfide oxidation calculations. This version underpredicted destruction of diethyl sulfide under all conditions. Ethylene levels were approximately correct for conditions with low destruction efficiencies, and significantly underpredicted under other conditions. CO levels were overpredicted by a large factor under conditions of low destruction, when CO levels were low. Agreement was better at higher destruction efficiency. Minor species C_2H_6 and CH_4 were consistently overpredicted. Carbon disulfide is underpredicted.

IV.B.7. Destruction pathways

Reaction pathway analysis was performed to identify the major reactions responsible for the creation and destruction of important species. The results are shown in Figures 20 and 21 for diethyl sulfide pyrolysis and oxidation, respectively.

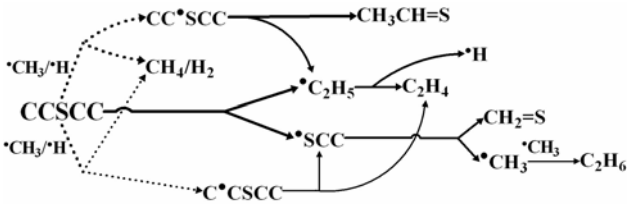

Fig. 20 Major reaction pathways for diethyl sulfide pyrolysis. Dotted lines indicate radical attack reactions. Thicker lines represent reactions with larger rates.

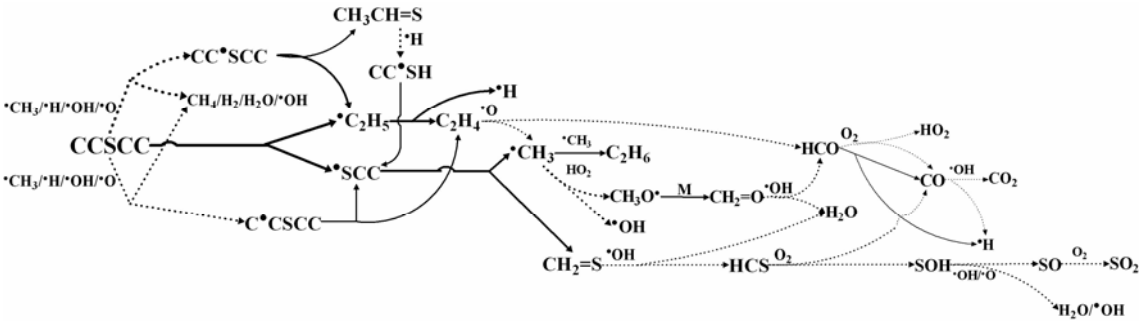

Fig. 21 Major reaction pathways for diethyl sulfide oxidation. Dotted lines indicate radical attack reactions. Thicker lines represent reactions with larger rates.

As the figures show, the destruction of diethyl sulfide proceeds through basically the same routes under both oxidative and pyrolytic conditions. Hydrogen abstraction by radicals creates one of two radicals, which then undergo beta scission. Alternatively, unimolecular dissociation can sever one of the C-S bonds of the parent molecule. The products of the dissociation reactions undergo beta scission.

V. REFERENCES

[1] M.K., Denison, C.J. Montgomery, A.F. Sarofim, M.J. Bockelie, A.G. Webster, R. Mellon, "Advanced Computational Modeling of Military Incinerators," presented at the Twenty-first International Conference on Incineration and Thermal Treatment Technologies, New Orleans, LA, May 13-17, 2002

[2] Sheng, C. Ph.D. Dissertation, Department of Chemical Engineering, New Jersey Institute of Technology, 2002.

[3] X. Zheng, E.M. Fisher, F.C. Gouldin, L. Zhu, and J.W. Bozzelli, 2008, "Experimental and Computational Study of Diethyl Sulfide Pyrolysis and Mechanism," accepted for publication, *Proceedings of the Combustion Institute*, v. 32.

[4] Reaction Design, 2004, Chemkin User Interface 4.0, available at http://www.reactiondesign.com.

[5] Wee Shong Chin, Bee Wai Ek, Chup Yew Mok, Hsing Hua Huang, J. Chem. Soc. Perkin Trans 2,(1994).